Raman Scattering Errors in Stimulated-Raman-Induced Logic Gates in ^{133}Ba$^+$

Matthew J. Boguslawski,[1,2,*,†] Zachary J. Wall,[1,*,‡] Samuel R. Vizvary,[1] Isam Daniel Moore,[3] Michael Bareian,[1] David T. C. Allcock,[3] David J. Wineland,[3] Eric R. Hudson,[1,2,4] and Wesley C. Campbell[1,2,4]

[1]*Department of Physics and Astronomy, University of California Los Angeles, Los Angeles, 90095 California, USA*
[2]*Challenge Institute for Quantum Computation, University of California Los Angeles, Los Angeles, 90095 California, USA*
[3]*Department of Physics, University of Oregon, Eugene, 97403 Oregon, USA*
[4]*Center for Quantum Science and Engineering, University of California Los Angeles, Los Angeles, 90095 California, USA*

(Received 13 January 2023; accepted 14 July 2023; published 7 August 2023)

^{133}Ba$^+$ is illuminated by a laser that is far detuned from optical transitions, and the resulting spontaneous Raman scattering rate is measured. The observed scattering rate is lower than previous theoretical estimates. The majority of the discrepancy is explained by a more accurate treatment of the scattered photon density of states. This work establishes that, contrary to previous models, there is no fundamental atomic physics limit to laser-driven quantum gates from laser-induced spontaneous Raman scattering.

DOI: 10.1103/PhysRevLett.131.063001

Trapped ion quantum systems have realized the highest-fidelity single- and two-qubit gate operations to date [1–5]. Nonetheless, these fidelities remain below estimated thresholds for realizing practical, fault-tolerant quantum computers [6]. As technical limitations on fidelity are overcome, it becomes increasingly important to understand any fundamental atomic physics limitations on gate fidelity, which is to say those that are inherent to a particular architecture.

For the case of stimulated-Raman laser-driven gates on trapped ion qubits, spontaneous emission error during gates is a chief source of infidelity. This process occurs when a far-off-resonant laser photon is incident and another photon is spontaneously emitted, resulting in the ion either returning to its initial state (spontaneous Rayleigh scattering) or transitioning to a different state (spontaneous Raman scattering, SRS) [7–13]. In SRS, the spontaneously emitted photon carries information about the ion internal state, thereby limiting the achievable fidelity. Spontaneous Rayleigh scattering can also effect two qubit gate fidelity, but to a lesser amount and was not a focus in this Letter [11,14].

Previous models of this process, here referred to as the constant density of states approximation (CDA) [9,10] posited the existence of a fundamental atomic physics lower limit $\varepsilon_{D\infty}$ to the achievable gate infidelity due to spontaneous scattering to the metastable ^2D_J states present in commonly used species. However, a recent treatment (referred to here as the "Moore *et al.* treatment") of photon scattering [14] that includes the frequency dependence of the density of states (see also Ref. [12]) predicts no such fundamental atomic physics limit.

In this Letter, we measure spontaneous Raman scattering of a trapped ^{133}Ba$^+$ ion qubit under laser illumination (Fig. 1). Our results disagree with CDA models of the scattering process, but agree with the Moore *et al.* treatment. In what follows, we detail a model of the scattering process that reproduces the main features of the experiment, describe the experimental approach and results, and discuss implications for trapped ion quantum information processing.

The salient features of the observed scattering rate can be understood with a model that stops short of the Moore *et al.* treatment. Using second-order perturbation theory, the scattering rate from initial state $|i\rangle$ (with energy $\hbar\omega_i$) to final state $|f\rangle$ ($\hbar\omega_f$) through the intermediate states $|k\rangle$ ($\hbar\omega_k$) can be estimated as

$$\Gamma_{i\to f} = \frac{\mathcal{E}_0^2}{4\hbar^2}\frac{\omega_{\rm sc}^3\Theta(\omega_{\rm sc})}{3\pi\epsilon_0\hbar c^3}\sum_q\left|\sum_k\frac{\langle f|d_q|k\rangle\langle k|d_\ell|i\rangle}{\omega_{ik}-\omega_\ell}\right|^2. \quad (1)$$

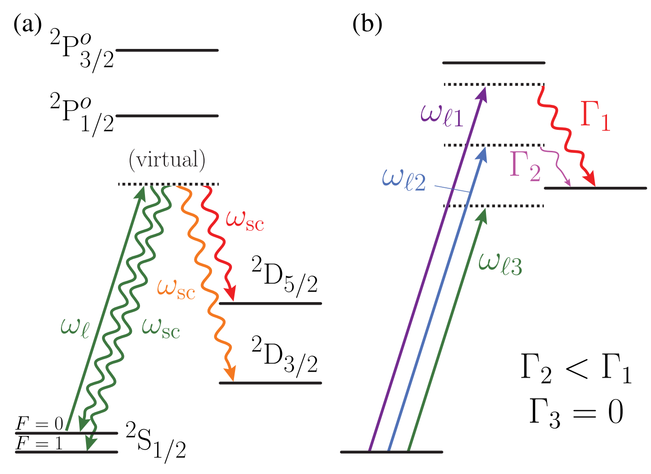

FIG. 1. (a) ^{133}Ba$^+$ level structure. The SRS photon frequency $\omega_{\rm sc}$ varies depending on the laser frequency ω_ℓ and the decay channel (wavy lines). (b) As the gate laser is detuned further to the red of the intermediate resonance ($\omega_{\ell i}$, $i = 1 \to 3$), the scattering rate to a metastable state (Γ_i, proportional to $\omega_{\rm sc}^3$) decreases until the error channel is closed [see $\omega_{\rm sc}^3\Theta(\omega_{\rm sc})$ in Eq. (1)].

Here, $\Theta(x)$ is the Heaviside step function; $\omega_{sc} \equiv \omega_\ell - \omega_{if}$ is the scattered photon frequency, given by the difference between the frequency of the incident laser photon ω_ℓ, and $\omega_{if} \equiv \omega_f - \omega_i$; $\omega_{ik} \equiv \omega_k - \omega_i$; $d_\ell \equiv \mathbf{d} \cdot \hat{e}_\ell$, and $d_q \equiv \mathbf{d} \cdot \hat{\mathbf{e}}_q$ are components of the electric dipole operator $\mathbf{d} \equiv \sum_j e\mathbf{r}_j$. The role of $\Theta(\omega_{sc})$ is to enforce energy conservation when the laser is too red to populate a particular potential final state via single-photon absorption [see Fig. 1(b)]. The applied laser, which we model as monochromatic, produces an electric field at the ion of $\mathbf{E}(t) = (\mathcal{E}_0/2)(\hat{e}_\ell e^{-i\omega_\ell t} + \hat{e}^*_\ell e^{i\omega_\ell t})$. The total spontaneous Raman scattering rate is calculated by summing Eq. (1) over all final states $|f\rangle$ with $f \neq i$, omitting Rayleigh scattering. The ratio of Rayleigh scattering error to Raman scattering error for two qubit gates in barium is roughly 5×10^{-3} and is not studied in this Letter [14]. Though this model, which we refer to as the ω^3-theory model, neglects emission-first processes, and we restrict our basis to the five lowest electronic states, it reproduces the observed scattering rate at the 10% level. Explicit expressions for the SRS rates in the CDA and ω^3-theory models in terms of Einstein A coefficients are given in Supplemental Material [15].

To empirically compare the scattering behavior of trapped ions in the far-detuned regime to these theories, we illuminate a trapped ion in a single initial quantum state with far-detuned light and probe for internal state changes induced due to SRS. Since far-off-resonance scattering is rare, high-fidelity state preparation and measurement (SPAM) is desirable to discern scattering from SPAM errors, and we accordingly perform this measurement with $^{133}Ba^+$ [4]. Specifically, a single $^{133}Ba^+$ ion [see Fig. 1(a)] is confined in a linear Paul trap with a minimum ion-electrode spacing of 3 mm driven at $\Omega = 2\pi \times 2.6$ MHz, resulting in a radial secular frequency of $\omega_r = 2\pi \times 230$ kHz. Ions are detected by imaging the laser induced fluorescence (LIF) of the $^2S_{1/2}$ to $^2P^o_{1/2}$ transition at 493 nm through an objective with a numerical aperture of 0.28. The ion is illuminated by a Continuum Verdi-V10, 532 nm laser focused to a $1/e^2$ intensity radius $w_0 \approx 40$ μm centered on the ion with optical power between 0.3 and 1.4 W. This wavelength is a suitable choice for driving gates in both $^2S_{1/2}$ g-type qubits and $^2D_{5/2}$ m-type qubits in $^{133}Ba^+$ [16]. The polarization of the light is set to drive σ^+ transitions, with a 0.5 mT magnetic field at the ion aligned antiparallel to the laser beam $\mathbf{k}$ vector [17]. The laser intensity is determined from a differential ac Stark shift measurement of the o-type clock-state qubit defined on $|^2S_{1/2}, F = 1, m_F = 0\rangle$ and $|^2D_{5/2}, F = 3, m_F = 0\rangle$ via narrow-linewidth optical spectroscopy at 1762 nm.

The total SRS rate measurement proceeds by first preparing the ion in the $|\uparrow\rangle \equiv |F = 0, m_F = 0\rangle$ g-type clock qubit state of the $^2S_{1/2}$ manifold via optical pumping [4]. The ion is then illuminated by the 532 nm laser for a chosen exposure time between 4 and 11 ms, during which the ion may spontaneously scatter a photon [see Fig. 1(a)]. Next, a 300 μs pulse of resonant 455, 585, and 650 nm light is used to optically pump ("shelve") the ion if it is in the $^2S_{1/2}(F = 1)$ or $^2D_{3/2}$ manifolds to $^2D_{5/2}$ with high fidelity [4]. Finally, population in $|\uparrow\rangle$ is measured by monitoring LIF while Doppler cooling via 493 and 650 nm illumination for 8 ms, and a measurement that does not yield LIF indicates that a SRS event occurred. An experimental pulse sequence diagram is shown in Supplemental Material [15]. The fraction of such "dark" events recorded in the same sequence without the 532 nm laser applied is subtracted from the laser-on experiments to yield a background-corrected probability of SRS events. Given the small probability of a SRS event, the experiment is repeated for $> 5 \times 10^4$ measurements to collect sufficient statistics, and the probability of multiple SRS events in a single illumination time is negligible. The SRS rate to only the $^2D_{5/2}$ manifold is measured in the same manner, omitting the shelving step. For the total SRS rate measurement, the observed background event probability was $6(2) \times 10^{-4}$, primarily due to shelving errors. As the measurement of scattering to $^2D_{5/2}$ requires no shelving step, background events are due primarily to state preparation errors, which occur with probability $4(4) \times 10^{-5}$. A detailed explanation of background events due to electron shelving is discussed in Supplemental Material [15].

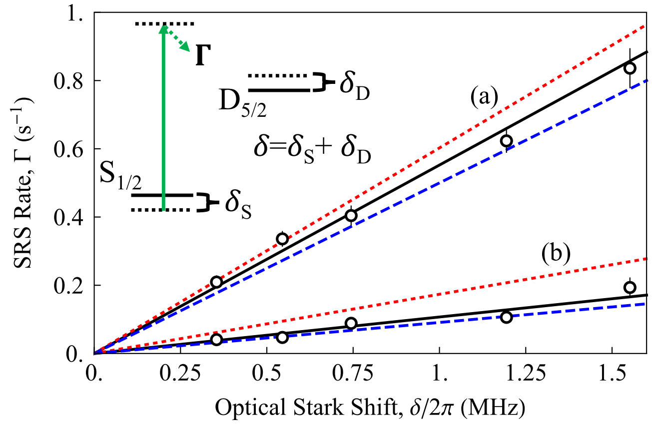

FIG. 2. SRS rate Γ from 532 nm laser illumination (green) versus differential o-type Stark shift δ. The upper grouping (a) shows the total SRS rate, while the lower grouping (b) shows rate for SRS into only $^2D_{5/2}$. Black circles: Measurements of the scattering rate. Red, dotted: CDA theory prediction. Black, solid: Moore *et al.* treatment. Blue, dashed: ω^3-theory prediction.

Figure 2(a) shows the measured total SRS rate plotted against the differential laser ac Stark shift of the o-type qubit and Fig. 2(b) shows the measured SRS rate into only the $^2D_{5/2}$ manifold. The scattering rate Γ_{meas} is extracted from the laser exposure time τ_ℓ, and the background-corrected, measured probability of scattering, P_{meas}, as

TABLE I. Comparison of models with the measured value of SRS rate vs laser intensity. Values are reported in units of SRS rate (10^{-9}) s^{-1} per (W/m^2) intensity.

SRS type	CDA	ω^3 [15]	Moore *et al.*	Measured
Total (Γ_{SRS})	1.65	1.37	1.52	1.52(5)
$D_{5/2}(\Gamma_{D_{5/2}})$	0.48	0.25	0.29	0.28(2)

$\Gamma_{meas} = -\ln(1 - P_{meas})/\tau_\ell$. The vertical error bars are calculated from the Wilson score interval for the measured scattering events [18]. The horizontal uncertainties are the standard errors of the spectral peak center of the optical spectra with and without the laser-induced Stark shift added in quadrature (smaller than the width of the data markers in Fig. 2).

A linear best fit is calculated using an orthogonal distance regression [19], taking into account statistical uncertainty in the measurements of the scattering rate and the Stark shift frequency. The Stark shift is calculated as a function of intensity and used to convert to laser intensity [9]. The results are summarized in Table I. The data show agreement within a standard error of the Moore *et al.* treatment of spontaneous Raman scattering. The ω^3-theory prediction for the total SRS rate shows a 10% offset due to the neglect of the emission-first terms that are present in the Moore *et al.* treatment. The measurements are in disagreement with the prediction of the CDA model, particularly for the SRS rate to ${}^2D_{5/2}$ states; this process produces a lower energy photon $\hbar\omega_{sc}$ than scattering to a ${}^2S_{1/2}$ state, leading to the observed larger deviation of the CDA from the data for the ${}^2D_{5/2}$ SRS process.

To explore this disagreement further, the SRS branching *fraction* to the ${}^2D_{5/2}$ manifold, $\eta_{D_{5/2}} \equiv \Gamma_{D_{5/2}}/\Gamma_{SRS}$ was separately measured, where $\Gamma_{D_{5/2}}$ and Γ_{SRS} are the ${}^2D_{5/2}$ and total SRS rates. Although the Stark shift of the laser was used to monitor the intensity stability on the ion, the result is independent of the intensity on the ion and is simply a function of the gate-laser wavelength. Figure 3 illustrates the striking consequence of the inclusion of the density of states ω_{sc}^3 factor (black trace). The CDA model (red dashed trace) shows a large asymptotic value of $\lim_{\omega_\ell \to 0} \eta_{D_{5/2}} = 0.73$, which implies nearly static fields would show a significant branching fraction to ${}^2D_{5/2}$, a consequence that would require violation of energy conservation. In contrast, the ω^3-theory model [Eq. (1)] shows scatter to ${}^2D_J$ smoothly becomes forbidden once the laser frequency is less than the ${}^2D_J$ transition frequency. The measured value of the SRS branching fraction $\eta_{D_{5/2}} = 0.19(1)$ is reproduced by the ω^3-theory model $(0.7\sigma_E)$, but is incompatible with the CDA model $(8.7\sigma_E)$—here σ_E is the standard error.

For quantum information applications, it is essential to understand the fundamental atomic physics limit posed by the far-detuned SRS events. For a stimulated-Raman transition, the probability of an ion to undergo an SRS event during the gate time τ_ℓ for gate lasers indexed by j is approximated by $\epsilon \approx 1 - e^{-\sum_j \tau_\ell \Gamma_j}$. For a typical single-qubit gate (modeled here as a π pulse) with two Raman beams, the gate time $\tau_{1q} = \pi/(2|\Omega_R|)$, where Ω_R is the resonant, stimulated-Raman Rabi frequency. For a two-qubit gate that traverses K loops in phase space, the gate time is reduced by the coupling strength to the motional sideband defined by the Lamb-Dicke parameter η, giving $\tau_{2q} = \pi\sqrt{K}/(2\eta|\Omega_R'|)$ [20]. For two-qubit gates, three beams may be used to produce two stimulated-Raman couplings, with the most efficient coupling realized in a counterpropagating configuration with two beams in one direction and the third, with twice the intensity in the opposite direction, increasing the Rabi rate Ω_R' by $\sqrt{2}$ compared to Ω_R for four balanced beams. The scattering rates Γ_j are given by Eq. (1), leading to single- and two-qubit gate errors of, respectively:

$$\epsilon_{1q} \approx 2\tau_{1q}\Gamma = \pi\Gamma/|\Omega_R|,$$
$$\epsilon_{2q} \approx (2)3\tau_{2q}\tilde{\Gamma} = 3\pi\sqrt{K}\tilde{\Gamma}/(\eta|\Omega_R'|). \quad (2)$$

Here, the expression for ϵ_{2q} accounts for the fact that SRS by either ion leads to an error, and $\tilde{\Gamma}$ is the scattering rate from the average beam intensity.

Since the stimulated-Raman Rabi frequency Ω_R is proportional to the differential ac Stark shift, the fit results from Fig. 2 can be used to calculate an empirical value for the achievable error probability for a two-qubit gate at

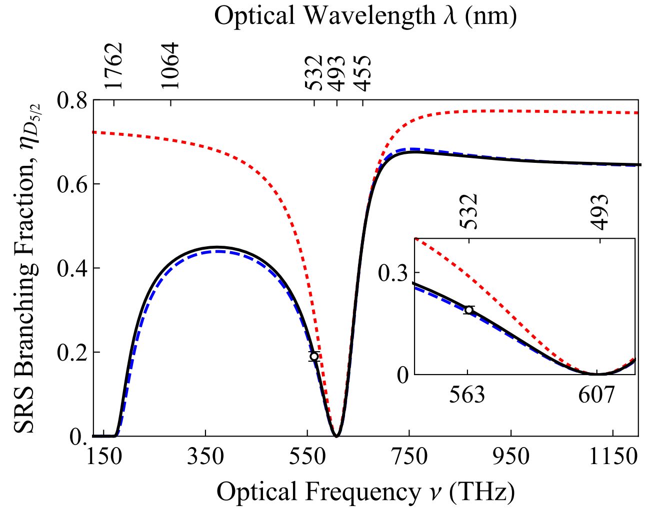

FIG. 3. The SRS branching fraction to the $D_{5/2}$ manifold $\eta_{D_{5/2}}$ as a function of laser frequency. Black, solid: Moore *et al.* treatment. Red, dotted: CDA model. Blue, dashed: ω^3-theory prediction. The black point shows the result of 21 measurements with the standard error displayed as error bars. The inset shows a close-up view near the gate-laser frequency.

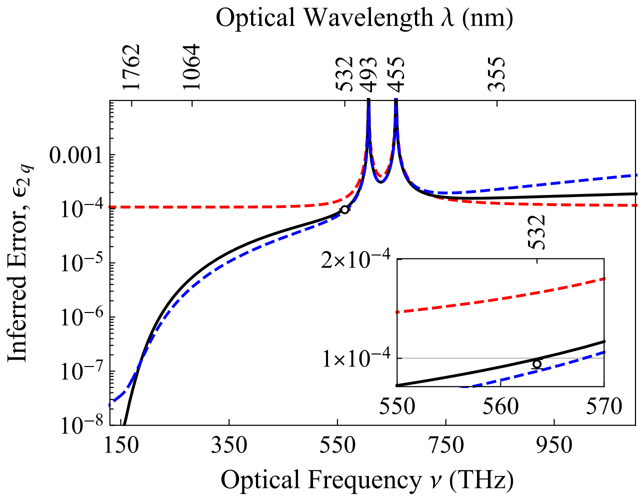

FIG. 4. Calculated two-qubit gate error versus gate-laser optical frequency. Black, solid: Moore *et al.* theory using a three-beam configuration, $K = 1$ and motional sideband frequency of $2\pi \times 5$ MHz. Red, dotted: CDA theory for three beams, which reproduces limit $\varepsilon_{D\infty} = (1/2)1.46 \times 10^{-4}$ for this configuration. Blue, dashed: ω^3-theory prediction. Black point: Inferred achievable two-qubit gate error, calculated from the measured scattering rate and Stark shifts at 532 nm.

532 nm [21]. In Fig. 4, we consider a two-qubit gate with $K = 1$ operating on a $2\pi \times 5$ MHz motional normal mode and find that the inferred two-qubit gate error is $6.4(2) \times 10^{-5}$, in agreement with the Moore *et al.* theory value of 6.6×10^{-5}. This is in contrast to the value provided in Table III of Ref. [10], where the CDA results in the conclusion that errors below $\varepsilon_{D\infty} = (1/2)1.46 \times 10^{-4} = 7.3 \times 10^{-5}$ (for a three beam configuration) detuned outside the ${}^2P_J^o$ levels are not possible in Ba^+ under *any* conditions. Further, for 532 nm, the CDA theory predicts an error of 1.05×10^{-4}, also in disagreement with our measurement-based estimate. Notably, the updated models as well as the infidelity inferred from measurements with a 532 nm gate laser reach below the 10^{-4} threshold anticipated for efficient error correction [6]. With the removal of the asymptotic error rate predicted by the CDA model, additional reductions to the SRS error rate can be found by, for example, choosing a gate laser further red detuned from the ${}^2P_J^o$ levels.

In summary, the Raman scattering rate of ${}^{133}Ba^+$ under illumination by laser light at 532 nm was studied and found to be smaller than previously predicted. The observed scattering rate agrees with more recent and more complete models, with the difference in models largely due to the inclusion of the scattered photon density of states. This result has important consequences. For example, in contrast with previous predictions for laser-based gates, there is no fundamental atomic physics limit to achievable gate error from spontaneous Raman scattering for trapped ion quantum processing since $\epsilon_{2q} \to 0$ as $\omega_\ell \to 0$. Also, in contrast with previous predictions [10], gate errors below 10^{-4} are achievable in ${}^{133}Ba^+$ at the technologically convenient wavelength of 532 nm.

We thank Clayton Ho for assistance in calculating Stark shifts and Roee Ozeri and Brian Sawyer for comments on the manuscript. This work was supported by the ARO under Grants No. W911NF-20-1-0037 and No. W911NF-19-1-0297 and the NSF under Grants No. PHY-2110421, No. PHY-2207985, and No. OMA-2016245.

[*]M. J. B. and Z. J. W. contributed equally to this work.
[†]mbog@physics.ucla.edu
[‡]zwall@physics.ucla.edu

[1] C. J. Ballance, T. P. Harty, N. M. Linke, M. A. Sepiol, and D. M. Lucas, Phys. Rev. Lett. **117**, 060504 (2016).
[2] J. P. Gaebler, T. R. Tan, Y. Lin, Y. Wan, R. Bowler, A. C. Keith, S. Glancy, K. Coakley, E. Knill, D. Leibfried, and D. J. Wineland, Phys. Rev. Lett. **117**, 060505 (2016).
[3] C. D. Bruzewicz, J. Chiaverini, R. McConnell, and J. M. Sage, Appl. Phys. Rev. **6**, 021314 (2019).
[4] J. E. Christensen, D. Hucul, W. C. Campbell, and E. R. Hudson, npj Quantum Inf. **6**, 35 (2020).
[5] C. R. Clark, H. N. Tinkey, B. C. Sawyer, A. M. Meier, K. A. Burkhardt, C. M. Seck, C. M. Shappert, N. D. Guise, C. E. Volin, S. D. Fallek, H. T. Hayden, W. G. Rellergert, and K. R. Brown, Phys. Rev. Lett. **127**, 130505 (2021).
[6] E. Knill, Nature (London) **434**, 39 (2005).
[7] M. B. Plenio and P. L. Knight, Proc. R. Soc. A **453**, 2017 (1997).
[8] D. J. Wineland, C. Monroe, W. M. Itano, D. Leibfried, B. E. King, and D. M. Meekhof, J. Res. Natl. Inst. Stand. Technol. **103**, 259 (1998).
[9] D. J. Wineland, M. Barrett, J. Britton, J. Chiaverini, B. DeMarco, W. M. Itano, B. Jelenković, C. Langer, D. Leibfried, V. Meyer, T. Rosenband, and T. Schätz, Phil. Trans. R. Soc. A **361**, 1349 (2003).
[10] R. Ozeri, W. M. Itano, R. B. Blakestad, J. Britton, J. Chiaverini, J. D. Jost, C. Langer, D. Leibfried, R. Reichle, S. Seidelin, J. H. Wesenberg, and D. J. Wineland, Phys. Rev. A **75**, 042329 (2007).
[11] H. Uys, M. J. Biercuk, A. P. VanDevender, C. Ospelkaus, D. Meiser, R. Ozeri, and J. J. Bollinger, Phys. Rev. Lett. **105**, 200401 (2010).
[12] B. C. Sawyer and K. R. Brown, Phys. Rev. A **103**, 022427 (2021).
[13] A. L. Carter, S. R. Muleady, A. Shankar, J. F. Lilieholm, B. B. Bullock, M. Affolter, A. M. Rey, and J. J. Bollinger, Phys. Rev. A **107**, 042618 (2023).
[14] I. D. Moore, W. C. Campbell, E. R. Hudson, M. J. Boguslawski, D. J. Wineland, and D. T. C. Allcock, Phys. Rev. A **107**, 032413 (2023).
[15] See Supplemental Material at http://link.aps.org/supplemental/10.1103/PhysRevLett.131.063001 for explicit formulas for scattering rates in terms of Einstein *A* coefficients.
[16] D. T. C. Allcock, W. C. Campbell, J. Chiaverini, I. L. Chuang, E. R. Hudson, I. D. Moore, A. Ransford, C. Roman, J. M. Sage, and D. J. Wineland, Appl. Phys. Lett. **119**, 214002 (2021).

[17] Beam polarization and bias field alignment was determined using measurements of polarization-dependent Stark shifts on the ion. Beam polarization was left-hand circular with a 99.86% degree of circular polarization at the vacuum viewport, measured with a Thorlabs PAX1000VIS polarimeter. The bias field was aligned to within an estimated 2° from the **k** vector axis.

[18] E. B. Wilson, J. Am. Stat. Assoc. **22**, 209 (1927).

[19] P. T. Boggs, R. H. Byrd, J. E. Rogers, and R. B. Schnabel, User's reference guide for ODRPACK version 2.01: Software for weighted orthogonal distance regression (1992), https://docs.scipy.org/doc/external/odrpack_guide.pdf.

[20] A. Sørensen and K. Mølmer, Phys. Rev. A **62**, 022311 (2000).

[21] The slope of the orthogonal distance regression of the total SRS data in Fig. 4 gives Γ/δ for SRS rate Γ and differential Stark shift δ. At 532 nm, δ/Ω_R is calculated following Eqs. 2.3 and 2.10 of [9]. Using this quantity, $\pi(\Gamma/\delta)(\delta/\Omega_R)(3\sqrt{K}/\eta) = (\Gamma/\Omega_R)(3\pi\sqrt{K}/\eta) = \epsilon_{2q}$ from Eq. (2) is calculated at 532 nm.